Closed-Loop Position and Cadence Tracking Control for FES-Cycling Exploiting Pedal Force Direction With Antagonistic Biarticular Muscles

Hiroyuki Kawai, *Member, IEEE*, Matthew J. Bellman, Ryan J. Downey, and Warren E. Dixon, *Fellow, IEEE*

***Abstract*— A functional electrical stimulation (FES)-based position and cadence tracking controller is developed to enable cycling by exploiting antagonistic biarticular muscles. A model of a stationary cycle and a rider is developed as a closed-chain mechanism. A strategy is then developed to switch between muscle groups based on the force direction of each muscle group. Stability of the developed controller is analyzed through Lyapunov-based methods. Experiments were conducted in seven healthy individuals and one individual with Parkinson's disease to illustrate the performance of the developed method. Specifically, the developed method was compared with voluntary tracking in terms of the position and velocity tracking errors. From the experimental results, we conclude that the proposed method can realize FES-cycling close to voluntary tracking.**

***Index Terms*— Functional electrical stimulation (FES), FES-cycling, Lyapunov stability, robust integral of the sign of the error (RISE)-based control.**

I. Introduction

The human body has been studied as a dynamical system for quite some time [1]–[4]. In healthy individuals, the coordinated firing of motor neurons activates skeletal muscles, which generate torques about the body's joints, thereby producing complex motions. However, neurological disorders that damage the motor neurons can lead to impaired motion. Specifically, people suffering from upper motor neuron disorders, such as stroke and spinal cord injury (SCI), have difficulty performing functional motions with affected limbs. Functional electrical stimulation (FES) seeks to augment lost motor neuron function through an artificially applied electric field to recover functional motion (e.g., stroke rehabilitation [5], tremor attenuation [6], walking [7], standing [8], grasping and releasing [9], and so on).

FES-cycling has been reported to be physiologically and psychologically beneficial for people suffering from disorders affecting the muscles of the lower limbs [10]; however, FES-cycling is metabolically inefficient and produces less power output than able-bodied cycling [11]. Previous studies have used various methods to address these shortcomings. Chen *et al.* [12] used a model-free fuzzy logic controller for FES-cycling. Gföhler and Lugner [13] considered an optimized stimulation pattern of leg muscles by FES. In [14], the influence of a number of individual parameters on the optimal stimulation pattern and power output during FES-cycling was investigated. van Soest *et al.* [15] considered a forward dynamics modeling/simulation approach to assess the potential effect of releasing the ankle on the maximal mechanical power output. Eser *et al.* [16] examined the relation between stimulation frequency and power output for cycling by trained SCI patients. Hunt *et al.* [17] proposed feedback control strategies for integration of electric motor assist and FES for paraplegic cycling. In [18], oxygen and stimulation costs were investigated to evaluate the effect on cycling performance. Kim *et al.* [19] proposed a feedback control system for FES-cycling, focusing on automatically determining stimulation patterns for multiple muscle groups. Ferrante *et al.* [20] investigated variable frequency stimulation patterns for increasing torque production and performance in FES-cycling. Ambrosini *et al.* [21] proposed the symmetry controller for FES-cycling, which is approximated by a discrete-time linear system. In [22], an automatic procedure to identify the session-specific stimulation parameters required during the training was designed for use in a clinical environment. Szecsi *et al.* [23] investigated the primary joints and muscles responsible for power generation and the role of antagonistic cocontraction in FES-cycling.

The aforementioned results provide promising methods for FES-cycling, though results are either empirical or use analytical methods from a theoretical perspective that are limited to linear approximations of the nonlinear cycle-rider system. Although linear approximations are suitable when the tracking error is sufficiently small, stability may not be guaranteed when the tracking error is large enough to induce significant approximation errors. Meanwhile, there are

Manuscript received April 24, 2017; revised October 18, 2017; accepted October 31, 2017. Date of publication December 6, 2017; date of current version February 8, 2019. Manuscript received in final form November 5, 2017. This work was supported in part by the Telecommunications Advancement Foundation, in part by JSPS KAKENHI under Grant 24760343 and Grant 15K06156, and in part by NSF under Award 1161260. Recommended by Associate Editor N. van de Wouw. *(Corresponding author: Hiroyuki Kawai.)*

H. Kawai is with the Department of Robotics, Kanazawa Institute of Technology, Nonoichi 921-8501, Japan (e-mail: hiroyuki@neptune.kanazawa-it.ac.jp).

M. J. Bellman and W. E. Dixon are with the Department of Mechanical and Aerospace Engineering, University of Florida, Gainesville, FL 32611-6250 USA.

R. J. Downey was with the Department of Mechanical and Aerospace Engineering, University of Florida, Gainesville, FL 32611-6250 USA. He is now with the College of Health Professions, Medical University of South Carolina, Charleston, SC 29425 USA.

Color versions of one or more of the figures in this paper are available online at http://ieeexplore.ieee.org.

Digital Object Identifier 10.1109/TCST.2017.2771727

1063-6536 © 2017 IEEE. Personal use is permitted, but republication/redistribution requires IEEE permission.
See http://www.ieee.org/publications_standards/publications/rights/index.html for more information.

additional complexities to be considered, since human motor control is a time-varying, nonlinear, many-to-one system [24]. Farhoud and Erfanian [25] proposed high-order sliding mode control scheme for the leg power in paraplegic FES-cycling. In [26], a robust controller was designed for FES-cycling, which is regarded as a switched control system. Some recent studies [27]–[29] have focused on the development of robust integral of the sign of the error (RISE)-based FES controllers and the associated analytical stability analysis for tracking of a human knee joint in the presence of a nonlinear uncertain muscle model with nonvanishing additive disturbances. However, these previous works have only considered single degree of freedom knee joint dynamics.

Based on the preliminary work in [30], this paper considers position and cadence tracking control for FES-cycling, derived using antagonistic biarticular muscles. Antagonistic biarticular muscles, which pass over two adjacent joints and therefore act on both joints simultaneously, are considered as one of the most important mechanisms of the human body associated with motion [31]–[33]. Based on the antagonistic biarticular muscle model, a stimulation pattern is derived for the gluteal, quadriceps femoris, hamstrings, and gastrocnemius muscle groups for a desired force profile (i.e., desired force direction as a function of the crank angle). In this paper, the stimulation pattern is derived with the goal of maintaining a tangential pedal force, which may improve power but not pedaling efficiency [34]; however, alternative stimulation patterns could similarly be developed for other desired force profiles to increase efficiency (e.g., setting the desired force profile to match that of an elite cyclist). The RISE-based controller and an associated stability analysis are developed for an uncertain nonlinear cycle-rider system by exploiting the force generation due to the antagonistic biarticular muscle groups. Toward this end, in this paper, a bicycle-rider model is developed that considers the input force mapping due to the antagonistic biarticular muscle groups in the lower body. Semiglobal asymptotic tracking of the desired trajectories is guaranteed, provided sufficient control gain conditions are satisfied. The developed controller was tested in seven healthy individuals and one individual with Parkinson's disease, expanding upon the theoretical work in [30].

This paper is organized as follows. In Section II, the bicycle model is represented as a closed-chain mechanism. In Section III, we develop the force direction at the pedal, and the stimulation pattern is determined for a desired force profile. The control development is presented in Section IV. Experimental results are shown in Section V on seven healthy participants to illustrate the performance of the developed method. An experiment is also provided in Section V on a person with Parkinson's disease to illustrate the applicability of the method in a person that would potentially be prescribed the FES-based cycling therapy. Concluding remarks are provided in Section VI.

II. Bicycle-Rider Model

A stationary cycle and a rider can be modeled as a closed-chain mechanism [35]. Consider a holonomic mechanical multibody system Σ' as shown in Fig. 1, which consists of a collection of rigid bodies described as

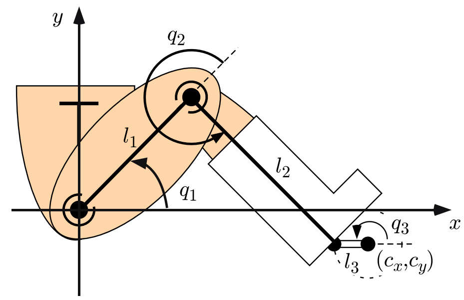

Fig. 1. Bicycle-rider model. The lengths of the thigh, shank, and crank are denoted by l_i $(i = 1, 2, 3)$; c_x and c_y are the coordinates of the center of the crank; and q_i $(i = 1, 2, 3)$ represent the hip, knee, and crank angles, respectively.

$$\Sigma' : \; M'(q')\ddot{q}' + C'(q', \dot{q}')\dot{q}' + g'(q') = 0 \tag{1}$$

where $q' = [q_1 \; q_2 \; q_3]^T \in \mathcal{R}^3$ represents the hip, knee, and crank angles, respectively, $M'(q') \in \mathcal{R}^{3\times3}$ is the inertia matrix, $C'(q', \dot{q}')\dot{q}' \in \mathcal{R}^3$ represents the centrifugal and Coriolis terms, and $g'(q') \in \mathcal{R}^3$ is the gravity term.

From Fig. 1, the scleronomic holonomic constraints are given by

$$\mathcal{C} : \; \phi(q') = \begin{bmatrix} l_1 C_1 + l_2 C_{12} - l_3 C_3 - c_x \\ l_1 S_1 + l_2 S_{12} - l_3 S_3 - c_y \end{bmatrix} = 0 \tag{2}$$

where l_i $(i = 1, 2, 3)$ are the lengths of the thigh, shank, and crank; c_x and c_y are the coordinates of the center of the crank; and S_i, S_{ij}, C_i, and C_{ij} are defined as $S_i := \sin(q_i)$, $S_{ij} := \sin(q_i + q_j)$, $C_i := \cos(q_i)$, and $C_{ij} := \cos(q_i + q_j)$, respectively.

Assumption 1: From (2) and the physical relationships associated with the seated cyclist, the hip and knee angles are constrained to the regions $\pi < q_2 < 2\pi$ and $\pi < q_1 + q_2 < 2\pi$.

In the subsequent development, the crank angle q_3 is assumed to be measurable. Other angles could be used without loss of generality; however, since the system is a closed-chain system and one angle can be used to fully describe all the angles, q_3 was selected because of the simplicity of measuring the crank angle. Hence, a parameterization for the generalized coordinates q is developed as

$$q' \longmapsto q = \alpha(q') = [0 \;\; 0 \;\; 1]]q'. \tag{3}$$

From [35, Th. 1], the equation of motion of the constrained system can be expressed in terms of the independent generalized coordinate q by combining

$$\begin{cases} M(q')\ddot{q} + C(q', \dot{q}')\dot{q} + g(q') = 0 \\ \dot{q}' = \mu(q')\dot{q} \\ q' = \sigma(q) \end{cases} \tag{4}$$

to yield

$$\Sigma : \; M(q)\ddot{q} + C(q, \dot{q})\dot{q} + g(q) = \tau \tag{5}$$

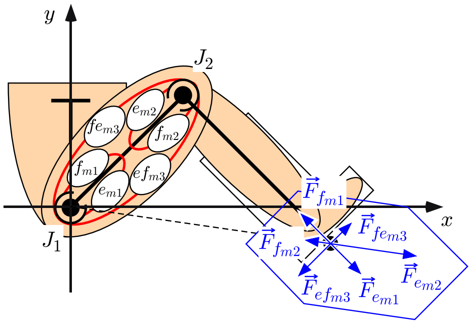

Fig. 2. Human thigh model. Antagonistic monoarticular muscles spanning the hip joint consist of three extensor muscles e_{m1}, i.e., gluteus maximus, gluteus medius, and gluteus minimus, and two flexor muscles f_{m1}, i.e., psoas major and iliacus. Antagonistic monoarticular muscles spanning the knee joint consist of biceps femoris short head f_{m2} and three extensor muscles e_{m2}, i.e., vastus intermedius, vastus lateralis, and vastus medialis. Antagonistic biarticular muscles spanning both the hip joint and the knee joint consist of rectus femoris fe_{m3} and three muscles ef_{m3}, i.e., biceps femoris long head, semimembranosus, and semitendinosus. The muscle fe_{m3} flexes the hip and extends the knee, while ef_{m3} extends the hip and flexes the knee.

where $\tau \in \mathcal{R}$ is the torque about the crank, $\mu(q')$ is expressed by using the constraints in (2) and the parameterization in (3), and $\sigma(q)$ can be derived by solving the constraints $\mathcal{C}$ in (2).

III. Input Force

Generally, a joint input torque can be generated by actuators in mechanical systems. However, it is difficult to directly apply traditional control design methods for mechanical systems to human motion control because of the nonlinear, time-varying, uncertain nature of human muscle. Thus, we first consider the effects of muscle contractions on the input torque at the crank. The human thigh model can be divided into three pairs of antagonistic muscles as shown in Fig. 2, where two groups consist of antagonistic monoarticular muscles and one group consists of antagonistic biarticular muscles. The antagonistic monoarticular muscles that span the hip joint consist of three extensor muscles denoted by e_{m1} and two flexor muscles denoted by f_{m1}. The antagonistic monoarticular muscles that span the knee joint consist of a flexor muscle denoted by f_{m2} and three extensor muscles denoted by e_{m2}. Antagonistic biarticular muscles span both the hip joint and the knee joint and consist of fe_{m3} and ef_{m3}, where fe_{m3} flexes the hip and extends the knee, and ef_{m3} extends the hip and flexes the knee.

The controllable resulting force at the pedal depends on the combination of the active muscle forces. Moreover, as shown in Fig. 2, the directions of $\vec{F}_{f_{m1}}$ and $\vec{F}_{e_{m1}}$ coincide with the direction of the shank and the direction of $\vec{F}_{f_{m2}}$ and $\vec{F}_{e_{m2}}$ pass through the hip joint J_1 and the pedal, and the directions of $\vec{F}_{fe_{m3}}$ and $\vec{F}_{ef_{m3}}$ are nearly parallel to the thigh as subsequently described. The torque produced at the joint(s) of the muscle spans is defined as

$$\tau_i := \Omega_i u_i, \quad \Omega_i := \zeta_i \eta_i \cos(a_i)$$
$$i \in \mathcal{T}, \quad \mathcal{T} := \{e_{m1}, f_{m1}, e_{m2}, f_{m2}, ef_{m3}, fe_{m3}\} \tag{6}$$

where $\zeta_i \in \mathcal{R}$ denotes a positive moment arm that changes with the crank angle [36], $a_i \in \mathcal{R}$ is defined as the pennation angle between the tendon and the muscle, which changes with the crank angle [27], $\eta_i \in \mathcal{R}$ is an unknown function that relates the applied voltage to muscle fiber force, which changes with the crank angle and velocity, and $u_i \in \mathcal{R}$ is the voltage control input applied across each muscle group.

Assumption 2: The moment arm ζ_i is assumed to be a positive, bounded, second-order differentiable function such that its first and second time derivatives are bounded if $q^k \in \mathcal{L}_\infty$, where q^k denotes the kth time derivative of q for $k = 0$, 1, and 2 [36]. Similarly, the function η_i is assumed to be a positive, bounded, second-order differentiable function such that its second time derivative is bounded if $q^k \in \mathcal{L}_\infty$ for $k = 0$, 1, 2, and 3 [37].

The forces at the pedal $F = [F_x \ F_y]^T$ are related to the joint torque $T = [T_1 \ T_2]^T$ as

$$F = (J^T)^{-1} T \tag{7}$$

where J is the Jacobian matrix[1] defined as

$$J := \begin{bmatrix} -l_1 S_1 - l_2 S_{12} & -l_2 S_{12} \\ l_1 C_1 + l_2 C_{12} & l_2 C_{12} \end{bmatrix}. \tag{8}$$

Moreover, the joint torques can be represented as

$$T_1 = (\tau_{f_{m1}} - \tau_{e_{m1}}) + (\delta_{f1} \tau_{fe_{m3}} - \delta_{e1} \tau_{ef_{m3}}) \tag{9}$$
$$T_2 = (\tau_{e_{m2}} - \tau_{f_{m2}}) + (\delta_{f2} \tau_{fe_{m3}} - \delta_{e2} \tau_{ef_{m3}}) \tag{10}$$

where $0 < \delta_{f1} \leq 1$, $0 < \delta_{f2} \leq 1$, $0 < \delta_{e1} \leq 1$, and $0 < \delta_{e2} \leq 1$ represent the ratio of the torque acting on each of the two joints (accounting for differences in moment arms) for each biarticular muscle, respectively. Using (7)–(10), the force at the pedal can be expressed as follows [38]:

$$|F_i| = \sqrt{F_{i_x}^2 + F_{i_y}^2} = R_i \tau_i \tag{11}$$
$$\theta_i = \tan^{-1}\left(\frac{F_{i_y}}{F_{i_x}}\right), \quad i \in \mathcal{T} \tag{12}$$

where

$$R_{f_{m1}} = \left|\frac{1}{l_1 S_2}\right|, \quad \theta_{f_{m1}} = q_1 + q_2 - \pi \tag{13}$$
$$R_{e_{m1}} = \left|\frac{1}{l_1 S_2}\right|, \quad \theta_{e_{m1}} = q_1 + q_2 \tag{14}$$
$$R_{f_{m2}} = \left|\frac{1}{l_2 S_0}\right|, \quad \theta_{f_{m2}} = \tan^{-1}\left(\frac{l_1 S_1 + l_2 S_{12}}{l_1 C_1 + l_2 C_{12}}\right) - \pi \tag{15}$$
$$R_{e_{m2}} = \left|\frac{1}{l_2 S_0}\right|, \quad \theta_{e_{m2}} = \tan^{-1}\left(\frac{l_1 S_1 + l_2 S_{12}}{l_1 C_1 + l_2 C_{12}}\right) \tag{16}$$

and R_i is a function that relates the torque and the generated force at the pedal, and θ_i is the direction of the force at the pedal.[2] Note that (15) and (16) make use of the geometric relationship $S_0 = -l_1 S_2/(l_1^2 + l_2^2 + 2l_1 l_2 C_2)^{1/2}$, where $q_0 := 2\pi - (q_1 + q_2) + \tan^{-1}((l_1 S_1 + l_2 S_{12})/(l_1 C_1 + l_2 C_{12}))$.

While healthy individuals may be able to activate individual muscles during voluntary contractions, it is difficult to selectively activate individual muscles during external FES with transcutaneous electrodes if the muscles are in close proximity

[1] $\det(J^T) = l_1 l_2 S_2 \neq 0$ except for $q_2 = n\pi$, $n \in \mathcal{Z}$. Thus, J^T is invertible under Assumption 1.

[2] If $\delta_{f1} = \delta_{f2} = 1$ and $\delta_{e1} = \delta_{e2} = 1$, then the directions of $\vec{F}_{fe_{m3}}$ and $\vec{F}_{ef_{m3}}$ are exactly parallel to the thigh, i.e., $\theta_{fe_{m3}} = q_1$ and $\theta_{ef_{m3}} = q_1 - \pi$.

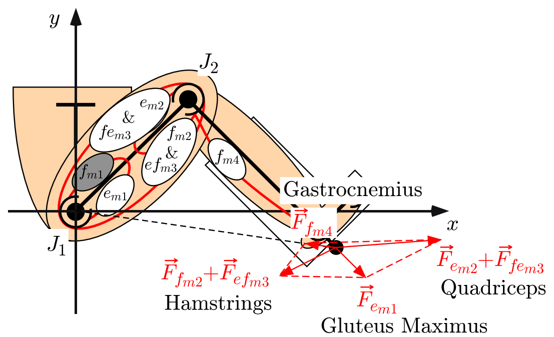

Fig. 3. Gastrocnemius is a biarticular muscle group, which is a flexor for the knee joint and is denoted as f_{m4}.

to each other. For example, it is difficult to separately activate e_{m2} (composed of the vastus intermedius, vastus lateralis, and vastus medialis) from fe_{m3} (the rectus femoris). It is also difficult to separately activate f_{m2} (the biceps femoris short head) from ef_{m3} (composed of the biceps femoris long head, the semimembranosus, and the semitendinosus). Moreover, deep muscles (e.g., psoas major and iliacus f_{m1}) cannot be activated by transcutaneous stimulation without also activating the superficial muscles. Therefore, we consider the quadriceps femoris muscle group, which contains e_{m2} and fe_{m3}, and the hamstrings muscle group which contains f_{m2} and ef_{m3} as shown in Fig. 3. Because the ankle joints of individuals undergoing physical therapy are often fixed rigidly during cycling for safety reasons, ankle flexion/extension is neglected in this paper. Thus, the gastrocnemius (typically biarticular) f_{m4} becomes a monoarticular flexor muscle for the knee joint and is used to modify the direction of force. Hereafter, we consider the following four muscle groups: gluteus maximus, hamstrings, gastrocnemius, and quadriceps.

The forces acting at the pedal for each muscle group are expressed as

$$\vec{F}_{\text{Glut}} = \vec{F}_{e_{m1}} \tag{19}$$
$$\vec{F}_{\text{Ham}} = \vec{F}_{f_{m2}} + \vec{F}_{ef_{m3}} \tag{20}$$
$$\vec{F}_{\text{Gast}} = \vec{F}_{f_{m4}} \tag{21}$$
$$\vec{F}_{\text{Quad}} = \vec{F}_{e_{m2}} + \vec{F}_{fe_{m3}} \tag{22}$$

where $\vec{F}_{f_{m4}}$ is similar to $\vec{F}_{f_{m2}}$ (i.e., $R_{f_{m4}} = R_{f_{m2}}$ and $\theta_{f_{m4}} = \theta_{f_{m2}}$), although the magnitudes of $\vec{F}_{f_{m4}}$ and $\vec{F}_{f_{m2}}$ are different (i.e., $|\vec{F}_{f_{m4}}| \neq |\vec{F}_{f_{m2}}|$). The crank torque can be expressed in terms of the muscle forces as

$$\tau = (\vec{F}_{\text{Glut}} + \vec{F}_{\text{Ham}} + \vec{F}_{\text{Gast}} + \vec{F}_{\text{Quad}}) \times \vec{l}_3 - d + M_e(q) + M_v(\dot{q}) \tag{23}$$

where $M_e(q) \in \mathcal{R}$ and $M_v(\dot{q}) \in \mathcal{R}$ are elastic [39] and viscous moments [40], respectively, defined as

$$M_e(q) := \mu(q')^T \begin{bmatrix} -k_{11}e^{-k_{12}q_1}(q_1 - k_{13}) \\ -k_{21}e^{-k_{22}q_2}(q_2 - k_{23}) \\ 0 \end{bmatrix} \tag{24}$$

$$M_v(\dot{q}) := \mu(q')^T \begin{bmatrix} b_{11}\tanh(-b_{12}\dot{q}_1) - b_{13}\dot{q}_1 \\ b_{21}\tanh(-b_{22}\dot{q}_2) - b_{23}\dot{q}_2 \\ 0 \end{bmatrix} \tag{25}$$

where $k_{11}, \ldots, k_{23} \in \mathcal{R}$ and $b_{11}, \ldots, b_{23} \in \mathcal{R}$ are unknown constants and $\vec{l}_3$ is defined as

$$\vec{l}_3 = l_3 \begin{bmatrix} C_3 \\ S_3 \end{bmatrix} \tag{26}$$

and d is an unknown bounded disturbance from unmodeled dynamics. Combining (5) and (23) yields

$$M(q)\ddot{q} + C(q,\dot{q})\dot{q} + g(q) = \left(\sum_{i \in \mathcal{S}} \vec{\Omega}_i u_i \times \vec{l}_3\right) - d + M_e(q) + M_v(\dot{q}) \tag{27}$$

where $\mathcal{S} = \{\text{Glut}, \text{Ham}, \text{Gast}, \text{Quad}\}$ and

$$\vec{\Omega}_{\text{Glut}} := R_{e_{m1}}\Omega_{e_{m1}} \begin{bmatrix} C_{12} \\ S_{12} \end{bmatrix} \tag{28}$$

$$\vec{\Omega}_{\text{Ham}} := R_{f_{m2}}\Omega_{f_{m2}} \begin{bmatrix} C\theta_{f_{m2}} \\ S\theta_{f_{m2}} \end{bmatrix} - R_{ef_{m3}}\Omega_{ef_{m3}} \begin{bmatrix} C\theta_{ef_{m3}} \\ S\theta_{ef_{m3}} \end{bmatrix} \tag{29}$$

$$\vec{\Omega}_{\text{Gast}} := R_{f_{m4}}\Omega_{f_{m4}} \begin{bmatrix} C\theta_{f_{m2}} \\ S\theta_{f_{m2}} \end{bmatrix} \tag{30}$$

$$\vec{\Omega}_{\text{Quad}} := R_{e_{m2}}\Omega_{e_{m2}} \begin{bmatrix} C\theta_{e_{m2}} \\ S\theta_{e_{m2}} \end{bmatrix} + R_{fe_{m3}}\Omega_{fe_{m3}} \begin{bmatrix} C\theta_{fe_{m3}} \\ S\theta_{fe_{m3}} \end{bmatrix}. \tag{31}$$

Given the natural muscle redundancy, a transformation is developed as

$$u_i = \chi_i u, \quad i \in \mathcal{S} \tag{32}$$

where $u \in \mathcal{R}$ is the subsequently developed control input, and $\chi_i \in [0,1]$ is the designed activation ratio used to control force direction. The position of the pedal exists inside of the quadrilateral, which is constructed by the force directions of the four muscle groups as shown in Fig. 4, and thus, the resulting force can be selected to be in any direction by altering the relative activation of the muscle groups. Because there exists infinitely many combinations by which three or more muscle groups can result in the same desired force direction, only two muscle

$$R_{fe_{m3}} = \frac{\sqrt{\delta_{f2}^2 l_1^2 + (\delta_{f1}^2 - \delta_{f2}^2) l_2^2 + 2(\delta_{f2} - \delta_{f1})\delta_{f2} l_2 (l_1 C_2 + l_2)}}{|l_1 l_2 S_2|}, \quad \theta_{fe_{m3}} = \tan^{-1}\left(\frac{(\delta_{f1} - \delta_{f2}) l_2 S_{12} - \delta_{f2} l_1 S_1}{(\delta_{f1} - \delta_{f2}) l_2 C_{12} - \delta_{f2} l_1 C_1}\right) \tag{17}$$

$$R_{ef_{m3}} = \frac{\sqrt{\delta_{e2}^2 l_1^2 + (\delta_{e1}^2 - \delta_{e2}^2) l_2^2 + 2(\delta_{e2} - \delta_{e1})\delta_{e2} l_2 (l_1 C_2 + l_2)}}{|l_1 l_2 S_2|}, \quad \theta_{ef_{m3}} = \tan^{-1}\left(\frac{(\delta_{e1} - \delta_{e2}) l_2 S_{12} - \delta_{e2} l_1 S_1}{(\delta_{e1} - \delta_{e2}) l_2 C_{12} - \delta_{e2} l_1 C_1}\right) - \pi \tag{18}$$

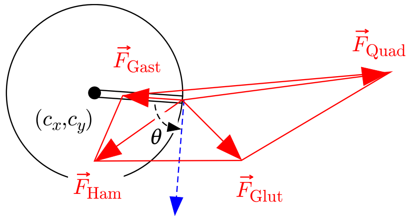

Fig. 4. Pedal force direction can be altered to lie within the quadrangle by varying the relative activation of each muscle group. As an example, the pedal force is desired to remain tangent to the crank in this paper. The goal of cadence tracking can be achieved, provided there is a nonzero control effectiveness (i.e., there must be a tangential component of the pedal force which causes the crank to move forward).

groups are activated at any given time in this approach.[3] The designed activation ratios are selected to satisfy the following relationships:

$$\chi_i + \chi_j = 1, \quad \chi_k = 0, \quad \chi_l = 0, \quad \sin\theta = 1 \tag{33}$$

where $(i, j) \in \{(\text{Glut}, \text{Ham}), (\text{Ham}, \text{Gast}), (\text{Gast}, \text{Quad}), (\text{Quad}, \text{Glut})\}$ and $(k, l) \in \mathcal{S} \neq i, j$, and θ is the angle between the direction of the combination of the muscle forces $\sum_{i\in\mathcal{S}} \chi_i \vec{\Omega}_i$ and the crank $\vec{l}_3$. The constraint on θ in (33) is designed such that the resulting combination of muscle forces is tangent to the crank, which may improve power but not pedaling efficiency. However, θ could also be prescribed as a function of the crank angle (e.g., that of a trained cyclist). By using (32), (27) can be expressed as

$$M(q)\ddot{q} + C(q,\dot{q})\dot{q} + g(q) - M_e(q) - M_v(\dot{q}) + d = \Omega_\chi u \tag{34}$$

where $\Omega_\chi = \| \sum_{i\in\mathcal{S}} \chi_i \vec{\Omega}_i \| l_3$.

To design χ_i and satisfy the constraint on θ in (33), the magnitude and direction must be known for $\vec{\Omega}_{\text{Glut}}$, $\vec{\Omega}_{\text{Ham}}$, $\vec{\Omega}_{\text{Gast}}$, and $\vec{\Omega}_{\text{Quad}}$. The directions of $\vec{\Omega}_{\text{Glut}}$ and $\vec{\Omega}_{\text{Gast}}$ can be obtained analytically as a function of the crank angle. However, $\vec{\Omega}_{\text{Ham}}$ and $\vec{\Omega}_{\text{Quad}}$ consist of multiple muscles where the force directions are known but the relative magnitudes of the forces are unknown, and thus, the directions of $\vec{\Omega}_{\text{Ham}}$ and $\vec{\Omega}_{\text{Quad}}$ have to be estimated numerically from experimental data. Furthermore, the relative magnitudes of $\vec{\Omega}_{\text{Glut}}$, $\vec{\Omega}_{\text{Ham}}$, $\vec{\Omega}_{\text{Gast}}$, and $\vec{\Omega}_{\text{Quad}}$ are unknown functions of the crank angle and crank velocity, and thus, the activation ratio χ_i must be designed based on experimental data.

Assumption 3: The first and second partial derivatives of χ_i with respect to the crank angle and crank velocity are assumed to exist and are bounded. Thus, from Assumption 2, the first and second partial derivatives of Ω_χ are bounded if $q^k \in \mathcal{L}_\infty$ for $k = 0$, 1, 2, and 3, and Ω_χ is assumed to be a bounded function.

From Assumption 2, Ω_i, $i \in \mathcal{T}'$, $\mathcal{T}' := \{e_{m1}, e_{m2}, f_{m2}, ef_{m3}, fe_{m3}, f_{m4}\}$ is bounded such that $\xi_i > \Omega_i > \varepsilon_i > 0$, $i \in \mathcal{T}'$ where ξ_i and $\varepsilon_i \in \mathcal{R}$ are positive constants. Furthermore, from Assumptions 1 and 2, Ω_χ is bounded such that $\xi_{\Omega_\chi} > \Omega_\chi > \varepsilon_{\Omega_\chi} > 0$ where ξ_{Ω_χ} and $\varepsilon_{\Omega_\chi} \in \mathcal{R}$ are positive constants.

[3]It is possible to stimulate three or more muscles per leg at any given time (e.g., distributing forces to reduce fatigue). However, a sufficient condition to guarantee cadence tracking is that the designed muscle activation profile should be sufficiently smooth (ON/OFF transition) and guarantee forward movement of the crank (nonzero tangential force).

IV. Control Development

The control objective is to enable the cycle crank to track a desired position and velocity to yield a desired pedaling motion. To quantify this objective, the crank position error is defined as

$$e_1 = q_d - q \tag{35}$$

where q_d is the desired crank angle, which is designed such that $q_d, q_d^k \in \mathcal{L}_\infty$, where q_d^k denotes the kth time derivative of q_d for $k = 1, 2, 3, 4$. To facilitate the subsequent analysis, the filtered tracking errors e_2, $r \in \mathcal{R}$ are defined as

$$e_2 = \dot{e}_1 + \alpha_1 e_1 \tag{36}$$

$$r = \dot{e}_2 + \alpha_2 e_2 \tag{37}$$

where α_1 and $\alpha_2 \in \mathcal{R}$ are selectable positive constants. By using (35)–(37), the crank dynamics in (34) can be transformed as follows:

$$\begin{aligned} M(q)r &= M(q)(\ddot{q}_d + \alpha_1\dot{e}_1 + \alpha_2 e_2) + C(q,\dot{q})\dot{q} \\ &\quad - M_e(q) - M_v(\dot{q}) + g(q) + d - \Omega_\chi u \\ &= W + d - \Omega_\chi u \end{aligned} \tag{38}$$

where W is defined as

$$\begin{aligned} W := M(q)(\ddot{q}_d + \alpha_1\dot{e}_1 + \alpha_2 e_2) + C(q,\dot{q})\dot{q} \\ - M_e(q) - M_v(\dot{q}) + g(q). \end{aligned} \tag{39}$$

After multiplying (38) by Ω_χ^{-1}, the following dynamics can be obtained:

$$M_\Omega(q,\dot{q})r = W_\Omega - u + d_\Omega \tag{40}$$

where $M_\Omega(q,\dot{q})$, W_Ω, and d_Ω are defined as

$$\begin{aligned} M_\Omega(q,\dot{q}) &:= \Omega_\chi^{-1} M(q), \\ W_\Omega &:= \Omega_\chi^{-1} W \\ &= M_\Omega(q,\dot{q})(\ddot{q}_d + \alpha_1\dot{e}_1 + \alpha_2 e_2) + C_\Omega(q,\dot{q})\dot{q} \\ &\quad - M_{e\Omega}(q,\dot{q}) - M_{v\Omega}(q,\dot{q}) + g_\Omega(q,\dot{q}) \\ d_\Omega &:= \Omega_\chi^{-1} d. \end{aligned}$$

From Assumptions 1–3 and the property that $\underline{M} \leq M(q) \leq \overline{M}$ where $\underline{M}$ and $\overline{M}$ are positive constants

$$\underline{M}_\Omega \leq M_\Omega \leq \overline{M}_\Omega \tag{41}$$

where $\underline{M}_\Omega$ and $\overline{M}_\Omega \in \mathcal{R}$ are positive constants. To facilitate the subsequent tracking control development, the following auxiliary terms are defined in terms of the desired trajectory:

$$\begin{aligned} S_d &:= M_{d\Omega}\ddot{q}_d + C_{d\Omega}\dot{q}_d - M_{ed\Omega} - M_{vd\Omega} + g_{d\Omega} + d_{d\Omega} \\ M_{d\Omega} &:= M_\Omega(q_d,\dot{q}_d), \quad C_{d\Omega} := C_\Omega(q_d,\dot{q}_d) \\ M_{ed\Omega} &:= M_{e\Omega}(q_d,\dot{q}_d), \quad M_{vd\Omega} := M_{v\Omega}(q_d,\dot{q}_d) \\ g_{d\Omega} &:= g_\Omega(q_d,\dot{q}_d), \quad d_{d\Omega} := d_\Omega(q_d,\dot{q}_d). \end{aligned}$$

To facilitate the stability analysis, the time derivative of (40) can be determined as

$$\begin{aligned} M_\Omega(q,\dot{q})\dot{r} &= -\dot{M}_\Omega(q,\dot{q})r + \dot{W}_\Omega - \dot{u} + \dot{d}_\Omega \\ &= -\frac{1}{2}\dot{M}_\Omega(q,\dot{q})r + N - \dot{u} - e_2 \\ &= -\frac{1}{2}\dot{M}_\Omega(q,\dot{q})r + \tilde{N} + N_d - \dot{u} - e_2 \quad (42) \end{aligned}$$

where N, N_d, and $\tilde{N} \in \mathcal{R}$ denote the following auxiliary terms:

$$\begin{aligned} N &:= \dot{W}_\Omega + e_2 - \frac{1}{2}\dot{M}_\Omega(q,\dot{q})r + \dot{d}_\Omega \\ N_d &:= \dot{S}_d \\ \tilde{N} &:= N - N_d. \end{aligned}$$

By applying the mean value theorem, $\tilde{N}$ can be upper bounded by state-dependent terms as

$$\|\tilde{N}\| \leq \rho(\|z\|)\|z\| \quad (43)$$

where $z \in \mathcal{R}^3$ is defined as

$$z := [e_1 \quad e_2 \quad r]^T \quad (44)$$

and $\rho(\|z\|)$ is a positive, nondecreasing radially unbounded function [41]. Since the desired trajectory is assumed to be bounded N_d and its time derivative can be upper bounded as

$$\|N_d\| \leq \zeta_{N_d}, \quad \|\dot{N}_d\| \leq \zeta_{\dot{N}_d} \quad (45)$$

where ζ_{N_d} and $\zeta_{\dot{N}_d} \in \mathcal{R}$ are known positive constants.

The control input is designed as [27]

$$u = (k_s + 1)(e_2 - e_2(0)) + \nu \quad (46)$$

$$\dot{\nu} = (k_s + 1)\alpha_2 e_2 + \beta \operatorname{sgn}(e_2), \quad \nu(0) = \nu_0 \quad (47)$$

where ν is the generalized Filippov solution to $\dot{\nu}$, ν_0 is some initial condition, k_s and $\beta \in \mathcal{R}$ are positive, constant control gains, and $\operatorname{sgn}(\cdot)$ denotes the signum function.

To facilitate the subsequent stability analysis, y and Q are defined as

$$y := \begin{bmatrix} z \\ \sqrt{P} \end{bmatrix}, \quad Q := \begin{bmatrix} \alpha_1 & -\frac{1}{2} & 0 \\ -\frac{1}{2} & \alpha_2 & 0 \\ 0 & 0 & 1 \end{bmatrix} \quad (48)$$

where $P \in \mathcal{R}$ is the Filippov solution to

$$\dot{P} = -r(N_d - \beta \operatorname{sgn}(e_2)) \quad (49)$$

$$P(0) = \beta|e_2(0)| - e_2(0)N_d(0). \quad (50)$$

Theorem 1: The controller in (46) yields semiglobal asymptotic tracking in the sense that

$$|e_1| \to 0 \quad \text{as } t \to \infty \quad (51)$$

for the region of attraction $\mathcal{D}_z$

$$\mathcal{D}_z = \left\{ y \mid \rho\left(\sqrt{\frac{\lambda_2}{\lambda_1}}\|y\|\right) < 2\sqrt{\lambda_{\min}(Q)k_s} \right\} \quad (52)$$

where $\lambda_1 := (1/2)\min\{1, \underline{M}_\Omega\}$, $\lambda_2 := \max\{(1/2)\overline{M}_\Omega, 1\}$, and $\lambda_{\min}(Q)$ denotes the minimum eigenvalue of Q, provided k_s is selected sufficiently large according to the initial conditions, and α_1, α_2, and β are selected according to the following sufficient conditions:

$$\alpha_1\alpha_2 > \frac{1}{4} \quad (53)$$

$$\beta > \left(\zeta_{N_d} + \frac{1}{\alpha_2}\zeta_{\dot{N}_d}\right) \quad (54)$$

where ζ_{N_d} and $\zeta_{\dot{N}_d}$ were introduced in (45).

Proof: By considering the following positive definite continuously differentiable function:

$$V(y) = \frac{1}{2}M_\Omega r^2 + \frac{1}{2}e_1^2 + \frac{1}{2}e_2^2 + P. \quad (55)$$

Theorem 1 can be proved based on the Lyapunov method [42]. For the details of the proof, please see Appendix C. □

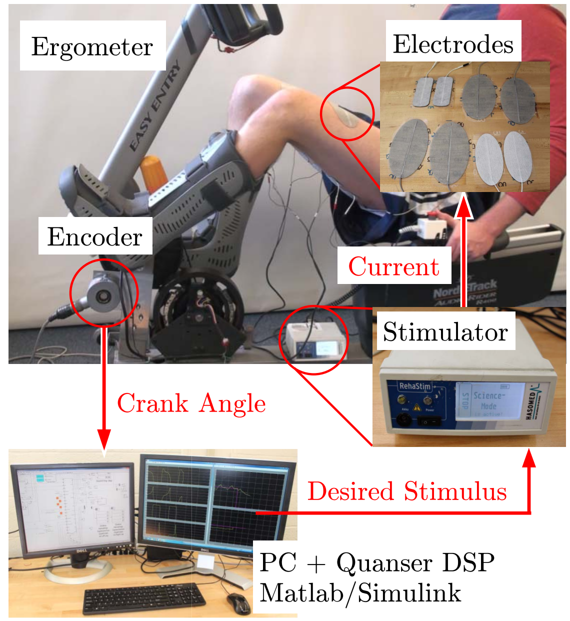

Fig. 5. FES-cycling system.

V. EVALUATION

A. Methods

1) Experimental Setup: The experimental setup is shown in Fig. 5. The ergometer was modified by attaching an encoder to measure the crank angle. A RehaStim current-controlled stimulator is used to deliver the developed controller. During the experiments, the stimulation frequency is fixed at 40 Hz, the developed control law determines the pulsewidth in real time, and the current amplitudes are fixed according to each participant. Two pairs of 3” by 5” oval PALS electrodes are placed over the quadriceps femoris and the hamstrings muscle groups. The gluteal and the gastrocnemius muscle groups have a pair of 2” by 4” oval StimTrode and a pair of 1.5” by 3.5” rectangle ValuTrode, respectively. Surface electrodes for the study were provided compliments of Axelgaard Manufacturing Co., Ltd. Control programs are written in MATLAB and Simulink, and implemented on a digital signal processor from Quanser using the Real-Time Workshop. A rebound air walker boot, produced by Össur, is attached at the pedal to fix the ankle joint rigidly.

2) Participants: Seven healthy males participated in the study in the age group of 24–41 years. An individual with Parkinson's disease, 60 years old with a unified Parkinson's disease rating scale (UPDRS) motor score of 12, total UPDRS score of 18, and modified Hoehn & Yahr score of 2.5, also participated in the study. Motivation to perform tests on healthy normal individuals was to demonstrate efficacy of the developed controller and to compare the performance of the external limb control method with volitional cycling. Note, as stated in [41]–[43], the response of muscle in individuals with a motor system disorder (e.g., SCI or Parkinson's disease) is essentially the same as the response by muscle in healthy normal individuals. Yet, there can be disease-specific differences (e.g., muscle spasticity). Therefore, to demonstrate efficacy in an example person with a motor system disorder, experiments were also performed in an individual with Parkinson's disease. Such an individual would be a candidate for FES-cycling therapy, based on the developed control approach.

3) Procedure: Prior to participating in the study, written informed consent was obtained from all participants, as approved by the Institutional Review Board at the University of Florida. Volunteers were instructed to relax as much as possible and to allow the stimulation to control the cycling motion (i.e., the subject was not supposed to influence the cycling motion voluntarily and was not allowed to see the desired trajectory). Both legs were stimulated by using the same control input u in (46), while the activation ratios on each muscle group of the right leg and the left leg have a 180 phase difference. The proposed method was compared with volitional cycling where each participant was able to see the velocity and position tracking error on a monitor. The participants were first asked to volitionally track the desired trajectory, given feedback of their tracking performance in the form of continuous trajectories plotted on a computer monitor. In addition, the participants were made aware that the desired speed would smoothly increase from 0 to 35 rpm in the beginning phase of every trial. The desired velocity was designed as $\dot{q}_d = -35(1 - e^{-0.25t})$ [rpm] $(= -3.67(1 - e^{-0.25t})$ [rad/s]). After the initial phase, the desired velocity tends to a constant, which is similar to the previous literature [22] for both volitional cycling and FES-cycling.[4] The gains were empirically selected as $k_s = 20$, $\alpha_1 = 0.21$, $\alpha_2 = 1.79$, and $\beta = 25$ for one subject and applied to all participants. In all experiments, the activation ratio χ_i, $i \in \mathcal{S}$, and $\mathcal{S} = \{\text{Glut}, \text{Ham}, \text{Gast}, \text{Quad}\}$ was determined as a function of the crank angle q by numerically solving (33) off-line based on the standard strength ratio of muscle groups for healthy males in [38] and the patient-specific kinematic parameters (i.e., c_x, c_y, and l_i, $i = 1, 2, 3$). These parameters are described in Appendix D.

4) Experimental Design and Data Analysis: The recorded data are separated into two periods, i.e., 0–10 cycles (until about 20 s) and 11–80 cycles (from about 20 s to about 140 s), as the transient and steady-state phases, respectively. Maximum steady-state error is defined as maximum absolute value of error during steady-state phase.

[4]As is typical in the literature, the experiments were performed for a constant desired cadence. However, the development in this paper can also be directly applied for any desired trajectory profile that is kinematically feasible/reasonable.

TABLE I
SUMMARIZED EXPERIMENTAL RESULTS FOR RMS POSITION ERROR

	Position Error (deg)					
	Tr RMS		SS RMS		Max	
Subject	RISE	Volu.	RISE	Volu.	RISE	Volu.
A	62.64	39.68	11.57	11.95	43.18	53.09
B	60.17	59.62	6.44	19.42	14.86	75.46
C	54.98	25.87	8.45	10.18	27.10	24.76
D	23.30	15.87	7.00	6.39	20.99	22.38
E	38.00	50.62	10.09	50.85	53.66	154.33
F	66.10	84.80	10.44	32.00	38.03	83.91
G	36.71	27.52	6.93	9.65	24.55	29.87
Mean	48.84	43.43	8.70	20.06	31.77	63.40
SD	16.18	23.67	2.02	16.07	13.69	46.97

TABLE II
SUMMARIZED EXPERIMENTAL RESULTS FOR RMS VELOCITY ERROR

	Velocity Error (RPM)					
	Tr RMS		SS RMS		Max	
Subject	RISE	Volu.	RISE	Volu.	RISE	Volu.
A	4.90	2.57	1.86	1.06	4.37	2.52
B	3.37	3.91	1.68	1.40	2.34	2.66
C	5.25	2.00	2.53	1.40	4.10	2.79
D	2.09	1.48	1.43	1.16	3.02	2.21
E	3.71	2.63	2.16	1.52	6.27	6.88
F	4.39	3.81	1.93	1.53	4.63	5.13
G	2.41	2.43	1.41	1.29	2.48	2.22
Mean	3.73	2.69	1.86	1.34	3.89	3.49
SD	1.20	0.89	0.40	0.18	1.39	1.81

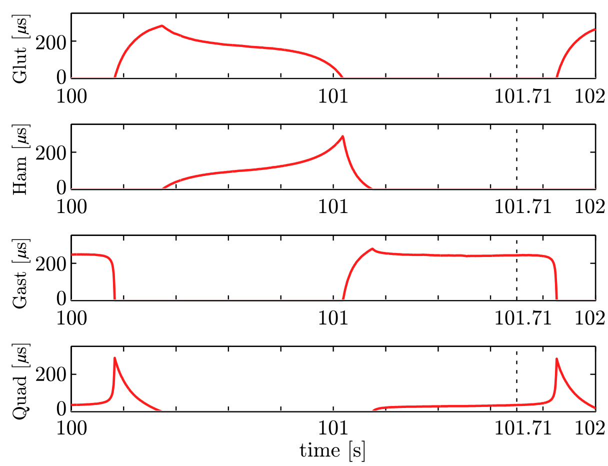

Fig. 6. Control inputs of one of the healthy participants where the developed controller was implemented. The single crank cycle is approximately 1.71 s (35 r/min).

B. Results

Tables I and II show experimental results for seven healthy participants. SD represents the standard deviation for each error. Tr, SS, rms, and Max refer to the transient phase, the steady-state phase, the root mean square, and the maximum steady-state error, respectively. Although rms velocity errors

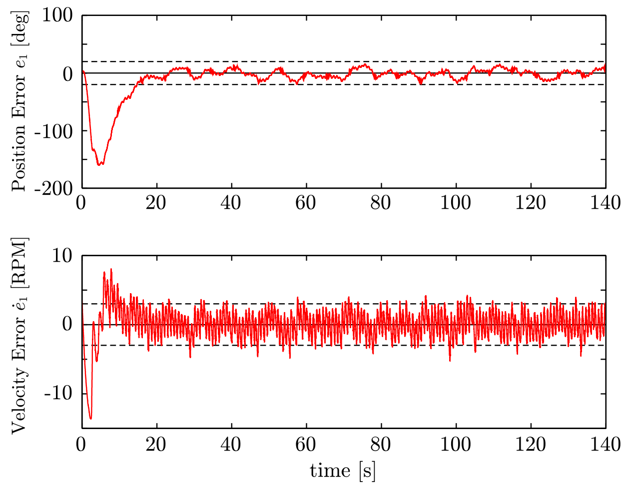

Fig. 7. Experimental results of one of the healthy participants where the developed controller was implemented. Dashed lines express ±20° and ±3 rpm for position error and velocity error, respectively.

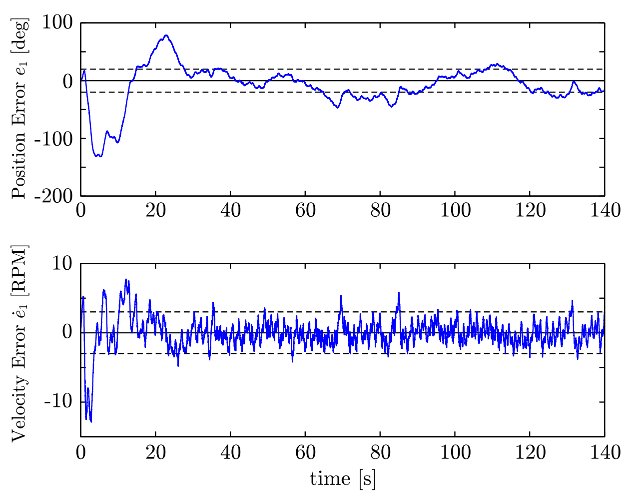

Fig. 8. Experimental results of one of the healthy participants during voluntary tracking. Dashed lines express ±20° and ±3 r/min for position error and velocity error, respectively.

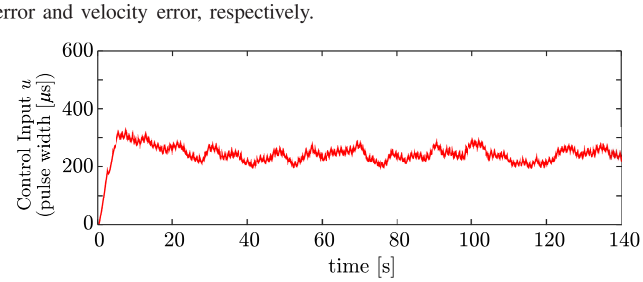

Fig. 9. Control input u of one of the healthy participants where the developed controller was implemented.

by the proposed method are slightly greater than voluntary tracking during the steady-state phase, these are very close individually. In addition, the proposed method reduced the rms position error for almost all the subjects during the steady-state phase. In conclusion, the proposed method can realize FES-cycling close to voluntary tracking from Tables I and II.

Fig. 6 shows the inputs for four muscle groups during a single crank cycle in the steady-state phase. These inputs are

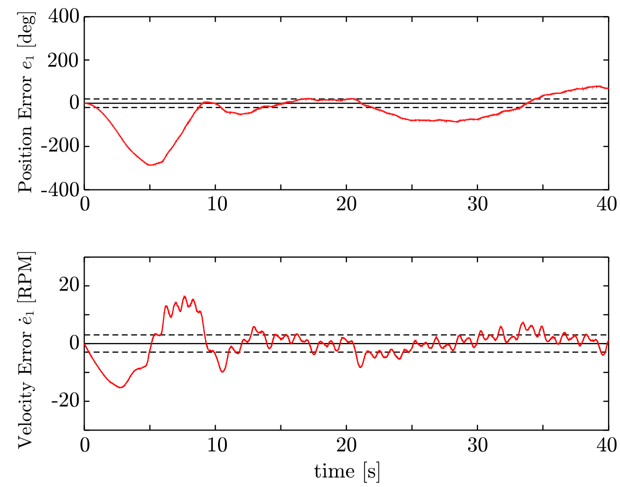

Fig. 10. Experimental results of the individual with Parkinson's disease where the developed controller was implemented. Dashed lines express ±20° and ±3 r/min for position error and velocity error, respectively.

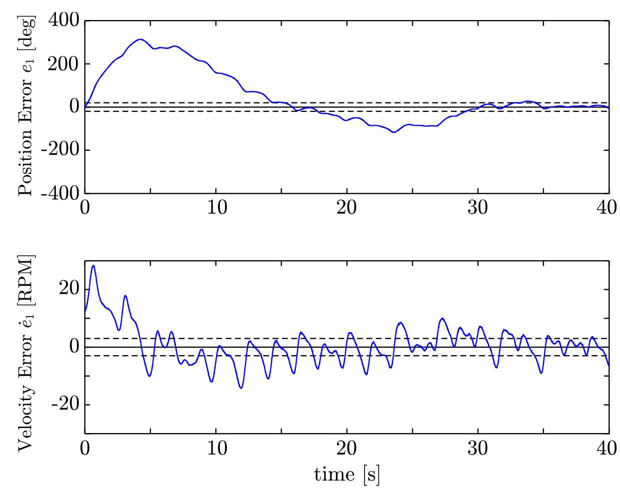

Fig. 11. Experimental results for the individual with Parkinson's disease during voluntary tracking. Dashed lines express ±20° and ±3 rpm for position error and velocity error, respectively.

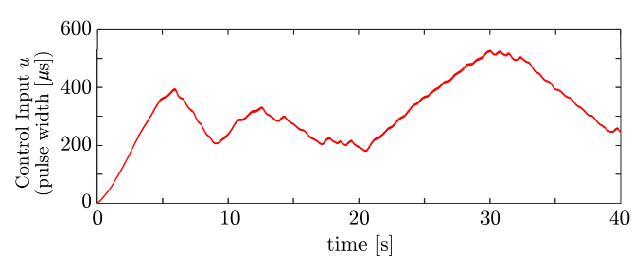

Fig. 12. Control input u of the individual with Parkinson's disease where the developed controller was implemented.

determined from the combination of the designed activation ratio χ_i, $i \in \mathcal{S}$, and $\mathcal{S} = \{\text{Glut}, \text{Ham}, \text{Gast}, \text{Quad}\}$ defined in (32), and the control input u defined in (46). Experimental results for the RISE-based controller and voluntary tracking are shown for one of the healthy participants in Figs. 7 and 8, respectively. Fig. 9 shows the control input u for a representative healthy participant. Although the velocity error with the

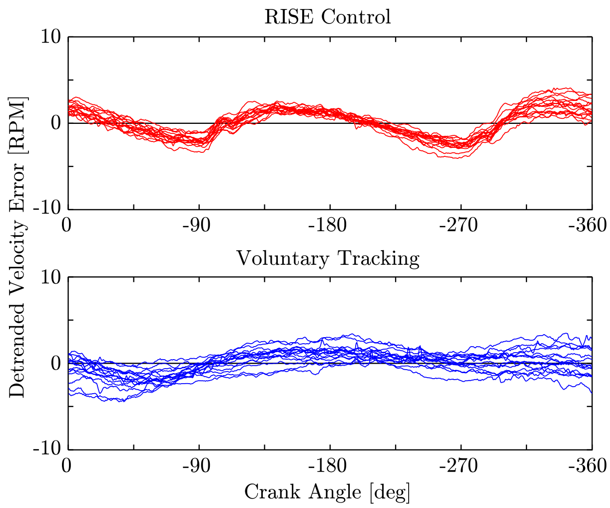

Fig. 13. Detrended velocity error of a healthy participant per cycle during cycles 6–20.

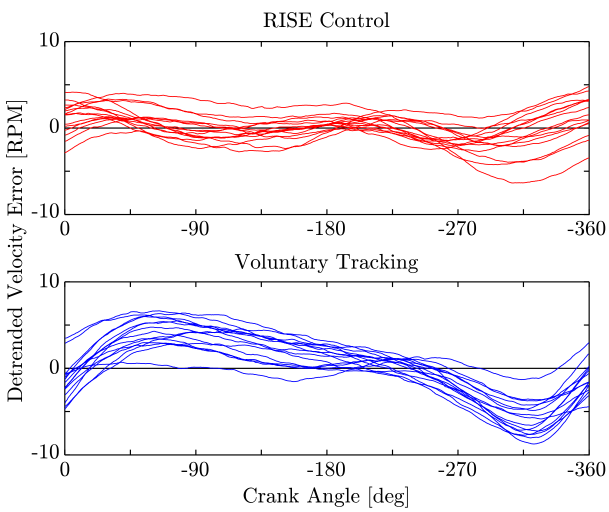

Fig. 14. Detrended velocity error of the Parkinson's disease patient per cycle during cycles 6–20.

developed controller has more oscillation than from voluntary tracking, FES-cycling with RISE control works sufficiently well for healthy participants. A demonstration video can be found on our Website [46].

Experimental results for the RISE-based controller and voluntary tracking are shown for the individual with Parkinson's disease in Figs. 10 and 11, respectively. Fig. 12 shows the control input u for the volunteer with Parkinson's disease. The individual with Parkinson's disease could not continue the experiment with the developed controller for more than 40 s because of control input saturation, which may have occurred due to a low threshold on the maximum allowable stimulation intensity that was implemented to maintain subject comfort. From Fig. 10 (bottom), the individual with Parkinson's disease could pedal with constant velocity by using the proposed method after 10 s. By comparing the velocity errors in Figs. 10 and 11, it can be seen that the voluntary tracking by the person with Parkinson's disease has large oscillation. To highlight any periodic trends in the velocity error as a function of the crank angle, the detrended velocity was plotted during cycles 6–20 for a healthy individual and the individual with Parkinson's disease in Figs. 13 and 14, respectively. The detrended velocity error was calculated by removing the mean value of the velocity error for each cycle. Fig. 13 shows two periods per one cycle, i.e., maximum velocity error appears at about $-135°$ and $-315°$, in both RISE control and voluntary tracking. However, we notice that voluntary tracking of the Parkinson's disease patient is asymmetric, i.e., the maximum and minimum velocity errors appear once per one cycle at about $-60°$ and $-315°$, respectively, as in Fig. 14 (bottom). Our proposed method reduced this asymmetry for velocity error, because the trend of velocity error was nearly flat in Fig. 14 (top).

VI. Conclusion

This paper considered closed-loop tracking control of an uncertain nonlinear cycle-rider system in the presence of an unknown time-varying disturbance (e.g., changing muscle characteristics induced by muscle fatigue). An RISE-based controller was developed to enable coordinated multilimb FES-cycling where a novel force vector mapping was used to exploit the effects of antagonistic biarticular muscles. An associated stability analysis guarantees semiglobal asymptotic tracking of the desired trajectory, provided sufficient control gain conditions are satisfied. Experimental results indicate that the developed FES-cycling controller can evoke position and cadence tracking (without visual aid or volitional effort) that is comparable to the tracking of healthy able-bodied individuals pedaling voluntarily while viewing the desired trajectory. Similarly, the results indicate that the controller has the potential to evoke the improved tracking performance (compared with volitional pedaling) in individuals with motor system disorders.

While the proposed method achieves good tracking performance for FES-cycling, pedal force sensors could be utilized in future work to measure the relative strength of each of the rider's muscle groups and provide insight into how the controller might be customized to accommodate the physiology of an individual rider. Such apparatuses could also provide direct feedback of the pedal force direction, for which a feedback controller could be designed. These investigations will be the subject of future work.

The objective of this paper was to develop an FES-cycling control system while considering the effects of antagonistic, biarticular muscle groups. The model and control development were generalized so that the control system can be applied to patient populations with various types and severities of neurological disorders (e.g., SCI, stroke, Parkinson's disease, and so on). Although the theoretical development is generalized, the practical implementation of the FES-cycling control system must account for the effects of a particular neurological disorder on the patient's physiology. For example, a spinal cord injured patient may have significant disuse atrophy that may exacerbate the rapid muscle fatigue induced by constant frequency, conventional FES. To account for this disorder-specific characteristic, the control system developed in this paper could be extended to include variable frequency or asynchronous stimulation, as in [47] and [48]. Similarly, a patient who is sensitive to or unfamiliar with FES, as was the case with the subject with Parkinson's disease in this paper, may require a lower preset maximum stimulation intensity to ensure subject comfort compared with other patients. Lower preset maximum stimulation intensities may lead to saturation of the stimulation input as greater evoked muscle force is required, thereby necessitating the extension of the developed control system to include saturated control methods [49]. Such extensions of the developed FES-cycling control system will be explored in future developments. While the development in this paper makes a contribution in developing a strategy utilizing antagonistic biarticulate muscles, several limitations remain. One topic for further investigation is methods to adaptively compensate for uncertain activation ratios for each person rather than identifying these ratios using pretrial experiments or using textbook ratios. In addition, by designing activation ratios that result in a pedal force profile similar to trained cyclists, future work could reexamine the developed controller in terms of metabolic efficiency.

Furthermore, in the particular case of the individual with Parkinson's disease, the controller was able to correct for an asymmetry in the individual's cycling cadence. These results highlight the potential of the developed controller to improve rehabilitative treatments; however, extended clinical trials in patient populations are required to understand the clinical efficacy of the proposed control method.

Appendix A
Reduced Model

Using the constraints in (2) and the parameterization in (3), let

$$\psi(q') := \begin{bmatrix} \phi(q') \\ \alpha(q') \end{bmatrix} = \begin{bmatrix} 0 \\ q \end{bmatrix}. \tag{56}$$

Differentiating (56) with respect to time yields

$$\psi_{q'}(q')\dot{q}' = [0 \quad 0 \quad 1]^T \dot{q} \tag{57}$$

where

$$\psi_{q'}(q') := \frac{\partial \psi(q')}{\partial q'} = \begin{bmatrix} -l_1 S_1 - l_2 S_{12} & -l_2 S_{12} & l_3 S_3 \\ l_1 C_1 + l_2 C_{12} & l_2 C_{12} & -l_3 C_3 \\ 0 & 0 & 1 \end{bmatrix}.$$

Therefore, $\mu(q')$ is obtained as

$$\mu(q') = \psi_{q'}^{-1}(q')[0 \quad 0 \quad 1]^T \tag{58}$$

where $\det(\psi_{q'}) = l_1 l_2 S_2 \neq 0$ except for $q_2 = n\pi,\ n \in \mathcal{Z}$. Thus, there exists $\psi_{q'}^{-1}(q')$ by Assumption 1, i.e., the knee joint angle q_2 never equals $n\pi,\ n \in \mathcal{Z}$.

By solving the constraints $\mathcal{C}$ in (2), q_1 and q_2 can be represented as functions of q_3 as

$$q_1 = \cos^{-1}\left(\frac{l_1^2 + (l_3 C_3 + c_x)^2 + (l_3 S_3 + c_y)^2 - l_2^2}{2 l_1 \sqrt{(l_3 C_3 + c_x)^2 + (l_3 S_3 + c_y)^2}}\right) + \tan^{-1}\left(\frac{l_3 S_3 + c_y}{l_3 C_3 + c_x}\right) \tag{59}$$

$$q_2 = \cos^{-1}\left(\frac{l_1^2 + l_2^2 - (l_3 C_3 + c_x)^2 - (l_3 S_3 + c_y)^2}{2 l_1 l_2}\right) + \pi. \tag{60}$$

The expressions in (59) and (60) yield the parameterization $\sigma(q)$.

Appendix B
Analytic Solution of q_3 for $\chi_{\mathrm{Glut}} = 1$ and $\chi_{\mathrm{Gast}} = 1$

This appendix develops analytic solutions of q_3 at $\chi_{\mathrm{Glut}} = 1$ and $\chi_{\mathrm{Gast}} = 1$. The crank angle which satisfies that $\vec{F}_{\mathrm{Glut}}$ and $\vec{l}_3$ cross at right angles is denoted by q_{Glut}. In other words, q_{Glut} equals q_3, which satisfies

$$q_3 - \frac{\pi}{2} = q_1 + q_2. \tag{61}$$

From (2) and (61)

$$q_{\mathrm{Glut}} = \sin^{-1}\left(\frac{l_3^2 + l_2^2 - l_1^2 + c_x^2 + c_y^2}{-2\sqrt{(c_y l_3 - c_x l_2)^2 + (c_x l_3 + c_y l_2)^2}}\right) - \varphi_1 + 2n\pi, \quad n \in \mathcal{Z} \tag{62}$$

where

$$\varphi_1 := \tan^{-1}\left(\frac{c_x l_3 + c_y l_2}{c_y l_3 - c_x l_2}\right) + \pi. \tag{63}$$

In a similar way, q_{Gast} is defined as a crank angle when $\vec{F}_{\mathrm{Gast}}$ and $\vec{l}_3$ cross at right angles. In other words, q_{Gast} equals q_3, which satisfies

$$q_3 - \frac{\pi}{2} = \tan^{-1}\left(\frac{l_1 S_1 + l_2 S_{12}}{l_1 C_1 + l_2 C_{12}}\right) = \tan^{-1}\left(\frac{l_3 S_3 + c_y}{l_3 C_3 + c_x}\right) \tag{64}$$

where (2) was utilized. From (64)

$$q_{\mathrm{Gast}} = \sin^{-1}\left(\frac{l_3}{-\sqrt{c_y^2 + c_x^2}}\right) - \varphi_2 + 2n\pi, \quad n \in \mathcal{Z} \tag{65}$$

where

$$\varphi_2 := \tan^{-1}\left(\frac{c_x}{c_y}\right) + \pi. \tag{66}$$

APPENDIX C
PROOF OF THEOREM 1

Proof: Integrating (49) indicates that

$$\begin{aligned}
&P(t) - P(0) \\
&= -\int_0^t \alpha_2 e_2(\tau)(N_d(\tau) - \beta \mathrm{sgn}(e_2(\tau)))d\tau \\
&\quad - \int_0^t \frac{d(e_2(\tau))}{d\tau}(N_d(\tau) - \beta \mathrm{sgn}(e_2(\tau)))d\tau \\
&= -\int_0^t \alpha_2 e_2(\tau)(N_d(\tau) - \beta \mathrm{sgn}(e_2(\tau)))d\tau \\
&\quad - e_2(\tau)N_d(\tau)|_0^t - \int_0^t e_2(\tau)\frac{dN_d(\tau)}{d\tau}d\tau + \beta|e_2(\tau)||_0^t \\
&= -\int_0^t \alpha_2 e_2(\tau)\left(N_d(\tau) + \frac{1}{\alpha_2}\frac{dN_d(\tau)}{d\tau} - \beta \mathrm{sgn}(e_2(\tau))\right)d\tau \\
&\quad - e_2(t)N_d(t) + e_2(0)N_d(0) + \beta|e_2(t)| - \beta|e_2(0)| \\
&= \int_0^t \alpha_2 e_2(\tau)\left(\beta \mathrm{sgn}(e_2(\tau)) - N_d(\tau) - \frac{1}{\alpha_2}\frac{dN_d(\tau)}{d\tau}\right)d\tau \\
&\quad - e_2(t)N_d(t) + e_2(0)N_d(0) + \beta|e_2(t)| - \beta|e_2(0)| \\
&\geq \int_0^t \alpha_2|e_2(\tau)|\left(\beta - |N_d(\tau)| - \frac{1}{\alpha_2}\left|\frac{dN_d(\tau)}{d\tau}\right|\right)d\tau \\
&\quad + |e_2(t)|(\beta - |N_d(t)|) - (\beta|e_2(0)| - e_2(0)N_d(0)). \qquad (67)
\end{aligned}$$

Based on the sufficient condition in (54), (50) and (67) indicate that $P(t) \geq 0$, and (55) satisfies the following inequalities:

$$\lambda_1\|y\|^2 \leq V \leq \lambda_2\|y\|^2. \qquad (68)$$

The time derivative of (55) exists almost everywhere (a.e.), i.e., for almost all $t \in [0, \infty)$, and $\dot{V} \overset{a.e.}{\in} \dot{\tilde{V}}$ where

$$\dot{\tilde{V}} := \bigcap_{\xi \in \partial V} \xi^T K\left[\dot{e}_1 \quad \dot{e}_2 \quad \dot{r} \quad \frac{1}{2}P^{-\frac{1}{2}}\dot{P} \quad 1\right]^T \qquad (69)$$

and ∂V is the generalized gradient of V. Since V is continuously differentiable, (69) can be rewritten as

$$\dot{\tilde{V}} \subset \nabla V^T K\left[\dot{e}_1 \quad \dot{e}_2 \quad \dot{r} \quad \frac{1}{2}P^{-\frac{1}{2}}\dot{P} \quad 1\right]^T \qquad (70)$$

where $\nabla V := \left[e_1 \quad e_2 \quad M_\Omega r \quad 2P^{\frac{1}{2}} \quad \frac{1}{2}\dot{M}_\Omega r^2\right]^T$. Using $K[\cdot]$ from [50], (70) yields

$$\begin{aligned}
\dot{\tilde{V}} &\subset e_1(e_2 - \alpha_1 e_1) + e_2(r - \alpha_2 e_2) \\
&\quad + r\Bigg(-\frac{1}{2}\dot{M}_\Omega(q)r + \tilde{N} + N_d - (k_s+1)\dot{e}_2 \\
&\qquad - (k_s+1)\alpha_2 e_2(t) - \beta K[\mathrm{sgn}(e_2)] - e_2\Bigg) \\
&\quad + K[\dot{P}] + \frac{1}{2}\dot{M}_\Omega r^2. \qquad (71)
\end{aligned}$$

By substituting $\dot{P}$ from (49), (71) can be transformed into

$$\begin{aligned}
\dot{\tilde{V}} &\subset e_1(e_2 - \alpha_1 e_1) - \alpha_2 e_2^2 + K[-r(N_d - \beta \mathrm{sgn}(e_2))] \\
&\quad + r(\tilde{N} + N_d - (k_s+1)r - \beta K[\mathrm{sgn}(e_2)]) \\
&= e_1(e_2 - \alpha_1 e_1) - \alpha_2 e_2^2 + r\beta K[\mathrm{sgn}(e_2)] \\
&\quad + r(\tilde{N} - (k_s+1)r - \beta K[\mathrm{sgn}(e_2)]). \qquad (72)
\end{aligned}$$

TABLE III

KINEMATIC PARAMETERS FOR ONE OF THE HEALTHY PARTICIPANTS

Crank center on x-axis c_x	0.7493 m
Crank center on y-axis c_y	−0.1905 m
Length of the thigh L_1	0.4699 m
Length of the shank L_2	0.5461 m
Length of the crank L_3	0.1714 m

Equation (72) can be further upper bounded as

$$\begin{aligned}
\dot{V} &\overset{a.e.}{\leq} -\alpha_1 e_1^2 + e_1 e_2 - \alpha_2 e_2^2 + r\tilde{N} - (k_s+1)r^2 \\
&= r\tilde{N} - k_s r^2 - z^T Q z \qquad (73)
\end{aligned}$$

where the set in (72) reduces to the scalar inequality in (73), because the right-hand side is continuous (a.e.), i.e., the right-hand side is continuous except for the Lebesgue negligible set of times when[5]

$$r(\beta K[\mathrm{sgn}(e_2)] - \beta K[\mathrm{sgn}(e_2)]) \neq \{0\}.$$

By using (43), the term $r^T\tilde{N}$ can be upper bounded as

$$\|r\tilde{N}\| \leq \rho(\|z\|)\|z\||r| \qquad (74)$$

to obtain

$$\dot{V} \overset{a.e.}{\leq} -\lambda_{\min}(Q)\|z\|^2 + \rho(\|z\|)\|z\||r| - k_s r^2. \qquad (75)$$

By completing the squares

$$\begin{aligned}
\dot{V} &\overset{a.e.}{\leq} -\lambda_{\min}(Q)\|z\|^2 - k_s\left(|r| - \frac{\rho(\|z\|)\|z\|}{2k_s}\right)^2 \\
&\quad + \frac{\rho(\|z\|)^2\|z\|^2}{4k_s} \\
&\leq -\left(\lambda_{\min}(Q) - \frac{\rho(\|z\|)^2}{4k_s}\right)\|z\|^2. \qquad (76)
\end{aligned}$$

From (76), it follows that:

$$\dot{V} \overset{a.e.}{\leq} -U = -\gamma\|z\|^2 \quad \forall y \in D \qquad (77)$$

where $\gamma \in \mathcal{R}$ is some positive constant, and $D := \{y \in \mathcal{R}^{3+1} \mid \rho(\|y\|) < 2(\lambda_{\min}(Q)k_s)^{1/2}\}$. From the inequalities in (68) and (77), $V \in \mathcal{L}_\infty$, and hence, e_1, e_2, and $r \in L_\infty$. The remaining signals in the closed-loop dynamics can be proven to be bounded. By invoking [52, Corollary 1], $\gamma\|z\|^2 \to 0$ as $t \to \infty$, $\forall y(0) \in \mathcal{D}_z$. Based on the definition of z, $e_1 \to 0$ as $t \to \infty$, $\forall y(0) \in \mathcal{D}_z$. The region of attraction D_z can be expanded arbitrarily by increasing k_s. □

APPENDIX D
PARAMETER IN EXPERIMENTS

In all experiments, we used the following ratio $e_{m1} : f_{m2} : e_{m2} : ef_{m3} : fe_{m3} : f_{m4} = 84 : 34 : 221 : 95 : 45 : 30$ for all subjects. Current amplitudes were adjusted for each participant based on pretrial data to prevent injuries and/or for comfort, e.g., Glut : Ham : Gast : Quad = 60 : 70 : 20 : 80 mA. For simplicity, we used $\delta_{f1} = \delta_{f2} = 1$ and $\delta_{e1} = \delta_{e2} = 1$ to obtain χ_i, $i \in \mathcal{T}'$ numerically in all subjects. The kinematic parameters for one of the participants are shown in Table III.

[5]See [51] for further details.

ACKNOWLEDGMENT

Any opinions, findings, and conclusions or recommendations expressed in this material are those of the authors and do not necessarily reflect the views of the sponsoring agencies.

REFERENCES

[1] G. Agarwal and G. Gottlieb, "Sampling in the human motor control system," *IEEE Trans. Autom. Control*, vol. AC-16, no. 2, pp. 180–183, Apr. 1971.

[2] H. Hatze, "Neuromusculoskeletal control systems modeling—A critical survey of recent developments," *IEEE Trans. Autom. Control*, vol. AC-25, no. 3, pp. 375–385, Jun. 1980.

[3] F. Previdi and E. Carpanzano, "Design of a gain scheduling controller for knee-joint angle control by using functional electrical stimulation," *IEEE Trans. Control Syst. Technol.*, vol. 11, no. 3, pp. 310–324, May 2003.

[4] R. D. Gregg and J. W. Sensinger, "Towards biomimetic virtual constraint control of a powered prosthetic leg," *IEEE Trans. Control Syst. Technol.*, vol. 22, no. 1, pp. 246–254, Jan. 2014.

[5] C. T. Freeman, E. Rogers, A.-M. Hughes, J. H. Burridge, and K. L. Meadmore, "Iterative learning control in health care: Electrical stimulation and robotic-assisted upper-limb stroke rehabilitation," *IEEE Control Syst.*, vol. 32, no. 1, pp. 18–43, Feb. 2012.

[6] J. Á. Gallego *et al.*, "A multimodal human–robot interface to drive a neuroprosthesis for tremor management," *IEEE Trans. Syst., Man, Cybern. C, Appl. Rev.*, vol. 42, no. 6, pp. 1159–1168, Nov. 2012.

[7] V. Nekoukar and A. Erfanian, "A decentralized modular control framework for robust control of FES-activated walker-assisted paraplegic walking using terminal sliding mode and fuzzy logic control," *IEEE Trans. Biomed. Eng.*, vol. 59, no. 10, pp. 2818–2827, Oct. 2012.

[8] R. Kamnik, J. Q. Shi, R. Murray-Smith, and T. Bajd, "Nonlinear modeling of FES-supported standing-up in paraplegia for selection of feedback sensors," *IEEE Trans. Neural Syst. Rehabil. Eng.*, vol. 13, no. 1, pp. 40–52, Mar. 2005.

[9] A. J. Westerveld, A. C. Schouten, P. H. Veltink, and H. van der Kooij, "Selectivity and resolution of surface electrical stimulation for grasp and release," *IEEE Trans. Neural Syst. Rehabil. Eng.*, vol. 20, no. 1, pp. 94–101, Jan. 2012.

[10] C.-W. Peng *et al.*, "Review: Clinical benefits of functional electrical stimulation cycling exercise for subjects with central neurological impairments," *J. Med. Biol. Eng.*, vol. 31, no. 1, pp. 1–11, 2011.

[11] K. J. Hunt, J. Fang, J. Saengsuwan, M. Grob, and M. Laubacher, "On the efficiency of FES cycling: A framework and systematic review," *Technol. Health Care*, vol. 20, no. 5, pp. 395–422, 2012.

[12] J. J. Chen, N.-Y. Yu, D.-G. Huang, B.-T. Ann, and G.-C. Chang, "Applying fuzzy logic to control cycling movement induced by functional electrical stimulation," *IEEE Trans. Rehabil. Eng.*, vol. 5, no. 2, pp. 158–169, Jun. 1997.

[13] M. Gföhler and P. Lugner, "Cycling by means of functional electrical stimulation," *IEEE Trans. Rehabil. Eng.*, vol. 8, no. 2, pp. 233–243, Jun. 2000.

[14] M. Gföhler and P. Lugner, "Dynamic simulation of FES-cycling: Influence of individual parameters," *IEEE Trans. Neural Syst. Rehabil. Eng.*, vol. 12, no. 4, pp. 398–405, Dec. 2004.

[15] A. J. van Soest, M. Gföhler, and L. J. Casius, "Consequences of ankle joint fixation on FES cycling power output: A simulation study," *Med. Sci. Sports Exercise*, vol. 37, no. 5, pp. 797–806, 2005.

[16] P. C. Eser, N. de N. Donaldson, H. Knecht, and E. Stüssi, "Influence of different stimulation frequencies on power output and fatigue during FES-cycling in recently injured SCI people," *IEEE Trans. Neural Syst. Rehabil. Eng.*, vol. 11, no. 3, pp. 236–240, Sep. 2003.

[17] K. J. Hunt *et al.*, "Control strategies for integration of electric motor assist and functional electrical stimulation in paraplegic cycling: Utility for exercise testing and mobile cycling," *IEEE Trans. Neural Syst. Rehabil. Eng.*, vol. 12, no. 1, pp. 89–101, Mar. 2004.

[18] K. J. Hunt *et al.*, "Comparison of stimulation patterns for FES-cycling using measures of oxygen cost and stimulation cost," *Med. Eng. Phys.*, vol. 28, no. 7, pp. 710–718, 2006.

[19] C.-S. Kim *et al.*, "Stimulation pattern-free control of FES cycling: Simulation study," *IEEE Trans. Syst., Man, Cybern. C, Appl. Rev.*, vol. 38, no. 1, pp. 125–134, Jan. 2008.

[20] S. Ferrante, T. Schauer, G. Ferrigno, J. Raisch, and F. Molteni, "The effect of using variable frequency trains during functional electrical stimulation cycling," *Neuromodulation, Technol. Neural Interface*, vol. 11, no. 3, pp. 216–226, 2008.

[21] E. Ambrosini, S. Ferrante, T. Schauer, G. Ferrigno, F. Molteni, and A. Pedrocchi, "Design of a symmetry controller for cycling induced by electrical stimulation: preliminary results on post-acute stroke patients," *Artif. Organs*, vol. 34, no. 8, pp. 663–667, 2010.

[22] E. Ambrosini, S. Ferrante, T. Schauer, G. Ferrigno, F. Molteni, and A. Pedrocchi, "An automatic identification procedure to promote the use of FES-cycling training for hemiparetic patients," *J. Healthcare Eng.*, vol. 5, no. 3, pp. 275–291, 2014.

[23] J. Szecsi, A. Straube, and C. Fornusek, "A biomechanical cause of low power production during FES cycling of subjects with SCI," *J. NeuroEng. Rehabil.*, vol. 11, no. 1, p. 123, 2014.

[24] A. Karniel and G. F. Inbar, "Human motor control: Learning to control a time-varying, nonlinear, many-to-one system," *IEEE Trans. Syst., Man, Cybern. C, Appl. Rev.*, vol. 30, no. 1, pp. 1–11, Feb. 2000.

[25] A. Farhoud and A. Erfanian, "Higher-order sliding mode control of leg power in paraplegic FES-cycling," in *Proc. 32nd Annu. Int. Conf. IEEE Eng. Med. Biol. Soc.*, Aug. 2010, pp. 5891–5894.

[26] M. J. Bellman, T.-H. Cheng, R. J. Downey, C. J. Hass, and W. E. Dixon, "Switched control of cadence during stationary cycling induced by functional electrical stimulation," *IEEE Trans. Neural Syst. Rehabil. Eng.*, vol. 24, no. 12, pp. 1373–1383, Dec. 2016.

[27] N. Sharma, K. Stegath, C. M. Gregory, and W. E. Dixon, "Nonlinear neuromuscular electrical stimulation tracking control of a human limb," *IEEE Trans. Neural Syst. Rehabil. Eng.*, vol. 17, no. 6, pp. 576–584, Dec. 2009.

[28] N. Sharma, C. M. Gregory, M. Johnson, and W. E. Dixon, "Closed-loop neural network-based NMES control for human limb tracking," *IEEE Trans. Control Syst. Technol.*, vol. 20, no. 3, pp. 712–724, May 2012.

[29] R. J. Downey, T.-H. Cheng, M. J. Bellman, and W. E. Dixon, "Closed-loop asynchronous neuromuscular electrical stimulation prolongs functional movements in the lower body," *IEEE Trans. Neural Syst. Rehabil. Eng.*, vol. 23, no. 6, pp. 1117–1127, Nov. 2015.

[30] H. Kawai, M. J. Bellman, R. J. Downey, and W. E. Dixon, "Tracking control for FES-cycling based on force direction efficiency with antagonistic bi-articular muscles," in *Proc. Amer. Control Conf.*, Jun. 2014, pp. 5484–5489.

[31] N. Hogan, "Impedance control: An approach to manipulation: Part I—Theory," *J. Dyn. Syst., Meas., Control*, vol. 107, no. 1, pp. 1–7, 1985.

[32] N. Hogan, "Impedance control: An approach to manipulation: Part II—Implementation," *J. Dyn. Syst., Meas., Control*, vol. 107, no. 1, pp. 8–16, 1985.

[33] N. Hogan, "Impedance control: An approach to manipulation: Part III—Applications," *J. Dyn. Syst., Meas., Control*, vol. 107, no. 1, pp. 17–24, 1985.

[34] D. J. J. Bregman, S. van Drongelen, and H. E. J. Veeger, "Is effective force application in handrim wheelchair propulsion also efficient?" *Clin. Biomech.*, vol. 24, no. 1, pp. 13–19, 2009.

[35] F. H. Ghorbel, O. Chetelat, R. Gunawardana, and R. Longchamp, "Modeling and set point control of closed-chain mechanisms: Theory and experiment," *IEEE Trans. Control Syst. Technol.*, vol. 8, no. 5, pp. 801–815, Sep. 2000.

[36] J. L. Krevolin, M. G. Pandy, and J. C. Pearce, "Moment arm of the patellar tendon in the human knee," *J. Biomech.*, vol. 37, no. 5, pp. 785–788, 2004.

[37] T. Watanabe, R. Futami, N. Hoshimiya, and Y. Handa, "An approach to a muscle model with a stimulus frequency-force relationship for FES applications," *IEEE Trans. Rehabil. Eng.*, vol. 7, no. 1, pp. 12–18, Mar. 1999.

[38] I. Nara *et al.*, *Biarticular Muscles: Motion Control and Rehabilitation*. Tokyo, Japan: Igaku-Shoin, 2008.

[39] M. Ferrarin and A. Pedotti, "The relationship between electrical stimulus and joint torque: A dynamic model," *IEEE Trans. Rehabil. Eng.*, vol. 8, no. 3, pp. 342–352, Sep. 2000.

[40] T. Schauer *et al.*, "Online identification and nonlinear control of the electrically stimulated quadriceps muscle," *Control Eng. Pract.*, vol. 13, no. 9, pp. 1207–1219, Sep. 2005.

[41] B. Xian, D. M. Dawson, M. S. D. Queiroz, and J. Chen, "A continuous asymptotic tracking control strategy for uncertain nonlinear systems," *IEEE Trans. Autom. Control*, vol. 49, no. 7, pp. 1206–1211, Jul. 2004.

[42] H. K. Khalil, *Nonlinear Control*, 3rd ed. Englewood Cliffs, NJ, USA: Prentice-Hall, 2002.

[43] G.-C. Chang *et al.*, "A neuro-control system for the knee joint position control with quadriceps stimulation," *IEEE Trans. Rehabil. Eng.*, vol. 5, no. 1, pp. 2–11, Mar. 1997.

[44] K. Kurosawa, R. Futami, TA. Watanabe, and N. Hoshimiya, "Joint angle control by FES using a feedback error learning controller," *IEEE Trans. Neural Syst. Rehabil. Eng.*, vol. 13, no. 3, pp. 359–371, Sep. 2005.

[45] J. M. Hausdorff and W. K. Durfee, "Open-loop position control of the knee joint using electrical stimulation of the quadriceps and hamstrings," *Med. Biol. Eng. Comput.*, vol. 29, no. 3, pp. 269–280, 1991.

[46] *Demonstration Videos*. Accessed: Nov. 14, 2017. [Online]. Available: http://wwwr.kanazawa-it.ac.jp/kawai/research/FES/FESvideos.html

[47] R. J. Downey, M. J. Bellman, N. Sharma, Q. Wang, C. M. Gregory, and W. E. Dixon, "A novel modulation strategy to increase stimulation duration in neuromuscular electrical stimulation," *Muscle Nerve*, vol. 44, no. 3, pp. 382–387, Sep. 2011.

[48] R. J. Downey, M. J. Bellman, H. Kawai, C. M. Gregory, and W. E. Dixon, "Comparing the induced muscle fatigue between asynchronous and synchronous electrical stimulation in able-bodied and spinal cord injured populations," *IEEE Trans. Neural Syst. Rehabil. Eng.*, vol. 23, no. 6, pp. 964–972, Nov. 2015.

[49] N. Fischer, Z. Kan, R. Kamalapurkar, and W. E. Dixon, "Saturated RISE feedback control for a class of second-order nonlinear systems," *IEEE Trans. Autom. Control*, vol. 59, no. 4, pp. 1094–1099, Apr. 2014.

[50] B. Paden and S. Sastry, "A calculus for computing Filippov's differential inclusion with application to the variable structure control of robot manipulators," *IEEE Trans. Circuits Syst.*, vol. CS-34, no. 1, pp. 73–82, Jan. 1987.

[51] R. Kamalapurkar, J. Klotz, R. J. Downey, and W. E. Dixon. (Jun. 2013). "Supporting lemmas for RISE-based control methods." [Online]. Available: https://arxiv.org/abs/1306.3432

[52] N. Fischer, R. Kamalapurkar, and W. E. Dixon, "LaSalle-Yoshizawa corollaries for nonsmooth systems," *IEEE Trans. Autom. Control*, vol. 58, no. 9, pp. 2333–2338, Sep. 2013.

Hiroyuki Kawai (M'04) received the B.Eng. degree in electrical and computer engineering from Kanazawa University, Kanazawa, Japan, in 1999, and the M.Eng. and Ph.D. degrees from the Graduate School of Natural Science and Technology, Kanazawa University, in 2001 and 2004, respectively.

From 2004 to 2005, he was a Post-Doctoral Scholar with the Information Technology Research Center, Hosei University, Tokyo, Japan. He was an Assistant Professor with the Kanazawa Institute of Technology, Nonoichi, Japan, from 2005 to 2010. From 2013 to 2014, he was a Visiting Scholar with the University of Florida, Gainesville, FL, USA. He is currently an Associate Professor with the Kanazawa Institute of Technology. His current research interests include the visual feedback control of robot systems, functional electrical stimulation-based human motion control, and passivity-based control.

Dr. Kawai was a recipient of the 2008 IEEE TRANSACTIONS ON CONTROL SYSTEMS TECHNOLOGY Outstanding Paper Award.

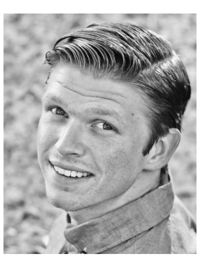

Matthew J. Bellman received the bachelor's and master's degrees (*magna cum laude*) in mechanical engineering with a minor in biomechanics and the Ph.D. degree in mechanical engineering as a National Defense Science and Engineering Fellow from the University of Florida, Gainesville, FL, USA.

He has been a member of the Nonlinear Controls and Robotics Group, University of Florida, since 2009. His current research interests include the theoretical development of robust, adaptive control systems for applications involving functional electrical stimulation, specifically those involving rehabilitation and mobility of the lower extremities.

Dr. Bellman was a recipient of the 2015 American Automatic Control Council O. Hugo Schuck (Best Paper) Award.

Ryan J. Downey received the B.S. degree in mechanical engineering from the University of Florida, Gainesville, FL, USA, in 2010, the first M.S. degree in biomedical engineering from the Politecnico di Milano, Milan, Italy, in 2012, and the second M.S. degree in biomedical engineering and the third M.S. and Ph.D. degrees in mechanical engineering from the University of Florida in 2012, 2014, and 2015, respectively.

He participated in the Research Experiences for Undergraduates Program at the University of Florida. In 2009, he joined the Nonlinear Controls and Robotics Group, University of Florida, as an Undergraduate Researcher. In 2011, he was accepted to an International Exchange Program (ATLANTIS CRISP) with the Politecnico di Milano. He is currently a Post-Doctoral Scholar with the Medical University of South Carolina, Charleston, SC, USA. His current research interests include functional electrical stimulation, Lyapunov-based nonlinear control, stroke, and sensory stimulation.

Dr. Downey was a recipient of the 2015 American Automatic Control Council O. Hugo Schuck (Best Paper) Award.

Warren E. Dixon (S'94–M'00–SM'05–F'16) received the Ph.D. degree from the Department of Electrical and Computer Engineering, Clemson University, Clemson, SC, USA, in 2000.

He was a Eugene P. Wigner Fellow with the Oak Ridge National Laboratory (ORNL), Oak Ridge, TN, USA, until 2004. In 2004, he joined the Mechanical and Aerospace Engineering Department, University of Florida, Gainesville, FL, USA, where he currently holds the Newton C. Ebaugh Professorship. His current research interests include the development and application of Lyapunov-based control techniques for uncertain nonlinear systems.

Dr. Dixon is an ASME Fellow and the IEEE Control Systems Society (CSS) Distinguished Lecturer. His work has been recognized by the 2015 and 2009 American Automatic Control Council O. Hugo Schuck (Best Paper) Award, the 2013 Fred Ellersick Award for the Best Overall MILCOM Paper, the 2012–2013 University of Florida College of Engineering Doctoral Dissertation Mentoring Award, the 2011 American Society of Mechanical Engineers (ASME) Dynamics Systems and Control Division Outstanding Young Investigator Award, the 2006 IEEE Robotics and Automation Society Early Academic Career Award, the NSF CAREER Award from 2006 to 2011, the 2004 Department of Energy Outstanding Mentor Award, and the 2001 ORNL Early Career Award for Engineering Achievement. He received the Air Force Commander's Public Service Award in 2016 for his contributions to the U.S. Air Force Science Advisory Board. He has served various editorial and other volunteer service positions, including the Director of Operations for the Executive Committee of the IEEE CSS Board of Governors from 2012 to 2015.